IDEA

Innovations Deserving
Exploratory Analysis Programs

Highway IDEA Program

Active Confinement of Bridge Piers Using Shape Memory Alloys

Final Report for Highway IDEA Project 135

Prepared by:
Bassem Andrawes, University of Illinois at Urbana-Champaign

February 2010

TRANSPORTATION RESEARCH BOARD
OF THE NATIONAL ACADEMIES

INNOVATIONS DESERVING EXPLORATORY ANALYSIS (IDEA) PROGRAMS MANAGED BY THE TRANSPORTATION RESEARCH BOARD (TRB)

This NCHRP-IDEA investigation was by Research & Technology Corp. completed as part of the National Cooperative Highway Research Program (NCHRP). The NCHRP-IDEA program is one of the three IDEA programs managed by the Transportation Research Board (TRB) to foster innovations in highway and intermodal surface transportation systems. The other two IDEA program areas are Transit IDEA, which focuses on products and results to advance transit practice in support of the Transit Cooperative Research Program (TCRP).

Safety IDEA Program, which focuses on innovative approaches for improving railroad safety and intercity bus and truck safety in support of the Federal Motor Carrier Safety Administration and the Federal Railroad Administration.

The three IDEA program areas are integrated to achieve the development and testing of nontraditional and innovative concepts, methods, and technologies, including conversion technologies from the defense, aerospace, computer, and communication sectors that are new to highway, transit, intelligent, and intermodal surface transportation systems.

For information on the IDEA Program contact IDEA Program, Transportation Research Board, 500 5th Street, N.W., Washington, D.C. 20001 (phone: 202/334-1461, fax: 202/334-3471, http://www.nationalacademies.org/trb/idea)

The project that is the subject of this contractor-authored report was a part of the Innovations Deserving Exploratory Analysis (IDEA) Programs, which are managed by the Transportation Research Board (TRB) with the approval of the Governing Board of the National Research Council. The members of the oversight committee that monitored the project and reviewed the report were chosen for their special competencies and with regard for appropriate balance. The views expressed in this report are those of the contractor who conducted the investigation documented in this report and do not necessarily reflect those of the Transportation Research Board, the National Research Council, or the sponsors of the IDEA Programs. This document has not been edited by TRB.

The Transportation Research Board of the National Academies, the National Research Council, and the organizations that sponsor the IDEA Programs do not endorse products or manufacturers. Trade or manufacturers' names appear herein solely because they are considered essential to the object of the investigation.

ACTIVE CONFINEMENT OF BRIDGE PIERS USING SHAPE MEMORY ALLOYS

IDEA Program Final Report

NCHRP-135

Prepared for the IDEA Program
Transportation Research Board
The National Academics

Bassem Andrawes
Department of Civil and Environmental Engineering
University of Illinois at Urbana-Champaign

February 23, 2010

ACKNOWLEDGEMENTS

The author would like to thank the Transportation Research Board (TRB), the National Academies, the National Cooperative Highway Research Program (NCHRP), and its Innovations Deserving Exploratory Analysis (IDEA) program for supporting this work. Special thanks to the NCHRP-IDEA committee and Dr. Inam Jawed for their guidance and invaluable comments and suggestions throughout the project.

TABLE OF CONTENTS

LIST OF FIGURES

LIST OF TABLES

EXECUTIVE SUMMARY

This IDEA project focused on developing an innovative *active* confinement technique for the seismic retrofitting of reinforced concrete (RC) bridge columns with insufficient ductility and/or shear capacity. The new technique utilizes a novel class of smart materials known as Shape Memory Alloys (SMAs) to provide external active confinement pressure at the plastic hinge zone of vulnerable columns. Wires made of NiTiNb SMAs are prestrained to approximately 6 %-strain then wrapped around the column in the form of spiral. Once the spiral is in place, it is heated to a temperature greater than the SMAs austenite transformation temperature (approximately 320 ^{o}F) and then left to cool. Heating the spirals can be done either directly using a torch or by simply passing an electrical current. Due to the *shape memory* effect of SMAs, heating the spirals will cause them to attempt to shrink to their original length, which will induce a large hoop stress in the spiral (≅ 65 ksi), which will in turn develop a lateral confining pressure on the perimeter of the column. Previous attempts to apply the concept of active confinement on bridge piers using steel and composite materials had all failed due to several problems related to the method of applying the confining pressure. This project provides a simple, reliable and cost-effective solution for these problems, which will facilitate and promote the application of active confinement which over performs the currently used passive confinement technique using steel jackets or fiber reinforced polymer (FRP) composites.

The work plan of this project comprised two main phases: (1) Material testing of SMA wires and confined concrete cylinders, and (2) Structural testing of reduced-scale RC columns retrofitted with SMA spirals. First, thermomechanical testing of 0.08 in.-diameter NiTiNb wires were conducted to determine their recovery stress. The tests revealed that the wires are capable of reaching a stable recovery stress of 67 ksi at room temperature. Spirals made of the NiTiNb wires were then used to confine 6 in. x 12 in. concrete cylinders. The cylinders were tested in compression to determine their uniaxial stress-strain behavior. Unconfined and glass-FRP (GFRP) wrapped cylinders were also tested and their behaviors were compared with the SMA-confined ones. Furthermore, a hybrid (passive + active) confinement technique was also investigated by wrapping the cylinders with GFRP sheets and SMA spirals. The results showed a significant increase in the strength and ultimate strain of SMA confined cylinders. Using 0.5 in. pitch spacing spiral increased the concrete strength and ultimate strain by 21 % and 24 times, respectively compared to that of unconfined concrete. Additionally, using the new hybrid confinement technique resulted in an improvement in the concrete ultimate strain by up to 30 times compared to that of the unconfined concrete. The small amount of SMAs used in the hybrid specimens played an important role in delaying the rupture of the GFRP sheets as well as the entire specimen in addition to maintaining up to 60 % of the concrete peak strength until failure. Further, under the same confinement pressure, SMA spirals resulted in about 1.2 and 10 times increase in the concrete strength and ultimate strain, respectively compared to GFRP wraps.

During the second phase of the project, and in order to examine the effectiveness of the new SMA spirals in improving the flexural ductility of RC bridge columns, four reduced-scale circular single cantilever RC columns were cast and tested under quasi-static lateral cyclic load. The diameter of the columns was 10 in. and their total height was 70 in. including the base. The columns were designed with insufficient lateral ductility. Three of the columns were retrofitted while the fourth column was tested in its as-built condition and used as the basis for the comparison. Each one of the three retrofitted columns was retrofitted at the plastic hinge zone using one of the techniques that were previously described, namely SMA spirals, GFRP jacket, and hybrid wraps (SMA + GFRP). The pitch of the SMA spirals and the thickness of the GFRP jackets were chosen so that the level of confinement pressure applied at the plastic hinge of the three retrofitted columns is the same. In addition to subjecting the columns to lateral loading, they were also subjected to a constant axial compression load during testing to represent the effect of dead load. The results indicated that the columns retrofitted with the SMA spirals were able to sustain larger force and drifts and dissipate significantly more hysteretic energy compared to that of the GFRP wrapped column. The displacement ductility ratio of the SMA column and the hybrid column was 2.4 times and 2.0 times that of the GFRP retrofitted column. Furthermore, the GFRP retrofitted column started showing significant signs of stiffness degradation and strength deterioration at a drift ratio of 5 %, while in the case of the SMA retrofitted column, no signs of degradation were observed until the column reached a drift ratio of 12 %. After removing the wrappings and cleaning up the crushed concrete, it was found that the columns retrofitted with SMA spirals showed the least damage among the four columns although they experienced 2.8 times and 1.75 times the maximum drift ratios sustained by the as-built and GFRP columns, respectively. This clearly demonstrated that using SMA spirals is not only effective in improving the flexural ductility of the columns, but also in limiting their damage during earthquakes, which will lead to a significant reduction in the level of repairs needed after a major earthquake.

1. IDEA PRODUCT

The product of this IDEA project is a NiTiNb SMA spiral that can be used for structural strengthening and remediation. Unlike traditional column retrofitting/repair methods (e.g. steel jackets and FRP wraps), these spirals are easy to use and require minimal on-site installation labor/time. The shape recovery feature of the spirals provides an easy solution for the problems commonly encountered during the application of active confinement on concrete using conventional materials. The ease of application provides perfect solution for problems where rapid actions are needed such as performing emergency post-earthquake or post-collision damage repairs. These spirals can easily ship to the site and get installed in a matter of a few hours. Furthermore, the tests conducted in this project clearly indicated the superiority of the new active confinement approach to conventional passive confinement using FRP jackets in terms of increasing the strength and flexural ductility of vulnerable columns as well as limiting the damage sustained by the columns under severe earthquakes. The SMA spirals examined and developed in this project will provide bridge engineers with a powerful tool to mitigate the effect of natural and man-made hazards on RC bridge systems.

2. CONCEPT AND INNOVATION

The concept of seismic retrofitting of RC bridge piers using active confinement had been previously tested using steel strands and fiber composite wraps and was compared to the conventional passive confinement approach. Experiments had proven with no doubt that active confinement is extremely more effective compared to passive confinement *(1)* However, practical application of active confinement in bridges has failed due to problems related to the technique used in applying the confining pressure using conventional materials (steel and composite). The proposed innovative approach relies on using the thermally activated shape memory feature of SMAs to apply active confinement in an easy, reliable and cost effective manner. The proposed approach will facilitate the application of active confinement and make it a more desirable retrofitting/repair method. This will directly enhance the performance of many RC bridges during earthquakes and also help maintain the functionality of transportation systems after major seismic events.

SMAs are a class of metallic alloys that exhibit the unique capability of recovering their original (undeformed) shape after being deformed. The shape recovery could be attained by heating the alloy to a temperature above the transformation temperature, A_f, which is a fixed property of the alloy predetermined by the user/manufacturer. The idea of using SMAs in providing active confinement for concrete is based on utilizing the recovery stress associated with the shape recovery of the SMAs when heated. This recovery stress could exceed 60 ksi depending on the material characteristics as well as on the level of deformation experienced prior to shape recovery *(2)*. Spirals made of NiTiNb SMAs will be manufactured and prestrained to about 6 %-strain. The SMA spirals will then be wrapped around the column at the most critical zone (e.g. plastic hinge) and heated using a torch or a electrical resistivity to a temperature above A_f. As the SMA spirals are heated above A_f, they will attempt to shrink back to their original length. Since the SMA spirals are anchored at both ends and the concrete column they are wrapped around is essentially incompressible, the induced shrinkage causes the SMA spirals to squeeze the concrete column. This squeezing effect provides the active confinement to the bridge pier columns. Figure 1 presents a schematic of the procedure proposed for applying active confinement to bridge piers using SMAs spirals. A key element in the success of this technique is the thermo-mechanical properties of the used SMAs. Although there are numerous SMA types, the NiTiNb alloy was particularly selected for this application due to its relatively wide thermal hysteresis. This will ensure that once the heating supply is cut and the spiral cools to typical ambient temperatures, it will not lose its recovery stress. It is worth mentioning that for the NiTiNb to loose its recovery stress, the temperature has to drop to below -58 ^oF, which is quite uncommon. Furthermore, the high A_f of the NiTiNb ($\approx$ 320 ^oF) is an important property which will prevent the spirals from recovering their original shapes during shipping or prior to being installed in the bridge.

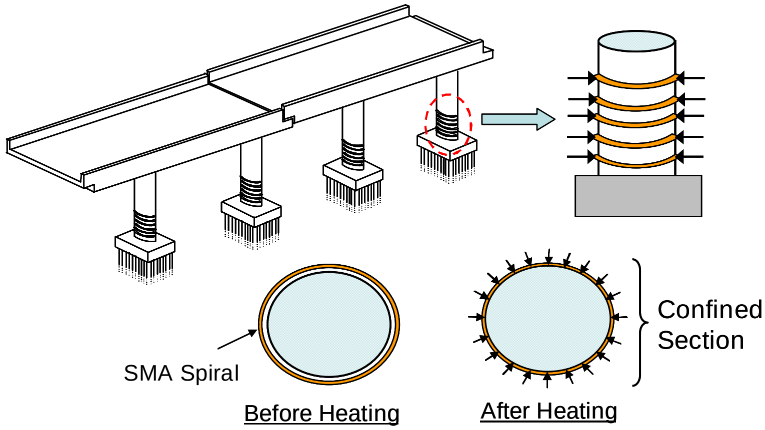

FIGURE 1 Schematic showing the procedure of using SMAs in actively confining RC bridge piers.

3. INVESTIGATION

3.1 RECOVERY STRESS TESTS OF SHAPE MEMORY ALLOYS

The first phase of the project focused on examining the recovery stress of NiTiNb SMA wires. The SMA wires used in the study were round with a cross section diameter of 0.08 in. They were provided by the manufacturer in a prestrained condition (approximately 6.4 % prestrain). In order to examine the recovery stress of the SMA wires at various temperatures, thermo-mechanical tests were conducted using a 20 kip MTS uniaxial servo-controlled hydraulic machine. In these tests, the SMA wire was clamped at both ends by the grips of the hydraulic frame then heated as shown in Figure 2. In order to ensure uniform distribution of the temperature throughout the entire length of the wire, it was heated by passing an electric current throughout its length. To monitor the wire's temperature during testing, a thermocouple was attached to the wire. Heating the SMA wire triggers its shape recovery, and since the wire was fully restrained, a recovery stress was induced in the wire. The recovery stress was calculated using the force measured by the load cell in the hydraulic machine.

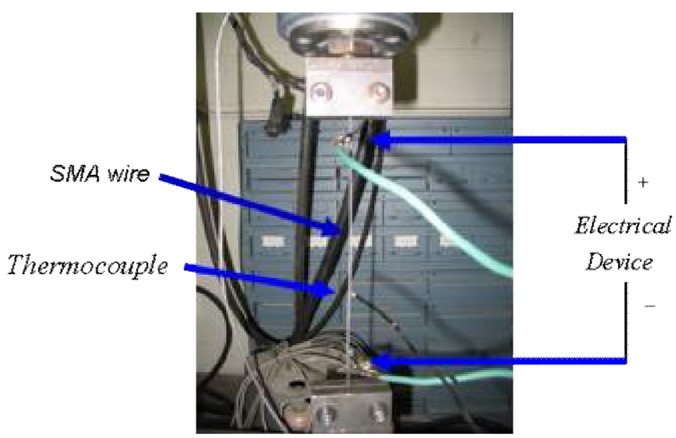

FIGURE 2 Recovery stress test of NiTiNb SMA wire.

Figure 3 shows the variation of recovery stress with time during the testing of the prestrained SMA wire (a) and the variation of the temperature with time (b). At the onset of heating, the recovery stress started increasing until it reached a maximum value of 82 ksi at a temperature of 264 ^{o}F. After which, the wire was left to cool. A slight decrease was observed in the recovery stress after the electric source was cut. The recovery stress became stable at a value of 67 ksi at room temperature (320 ^{o}F).

In order to examine the relationship between the level of the recovery stress induced by heating and the prestrain value, the same recovery stress test described above was conducted on three SMA wire specimens. The three specimens were prestrained to different strain values of approximately 6.4 %, 4.5 % and 2.8%. Figure 4 shows the relationship between the recovery stresses (maximum and residual) and the prestrain value. As shown in the figure, the recovery stress induced in the wires increased linearly with the amount of prestrain. When the level of prestrain of the wire increased from 2.8% to 6.4%, the maximum recovery stress increased by 22 %, and the residual recovery stress increased by 17 %. In general it was observed that the average residual recovery stress was approximately 80% of the maximum recovery stress.

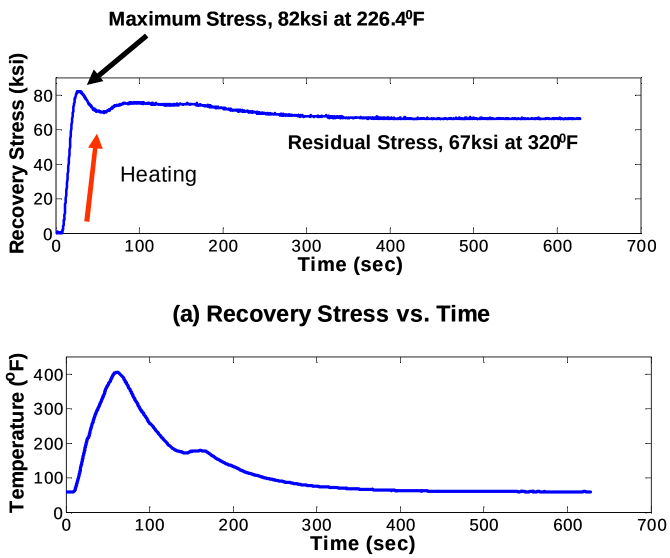

(b) Temperature vs. Time

FIGURE 3 Recovery stress induced in the SMA wire vs. time (a), and the variation of the temperature vs. time (b).

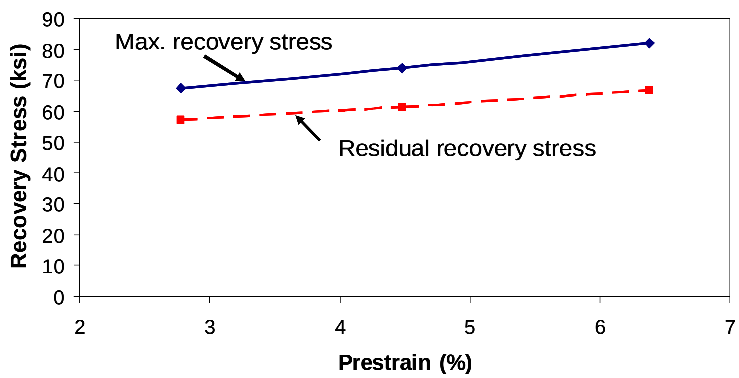

FIGURE 4 Relationship between recovery stress induced in the SMA wire and its prestrain value.

To examine the mechanical behavior of the prestressed SMA wires after reaching a stable recovery stress, the wires were subjected to cyclic loading. The displacement-controlled cyclic load was applied with a strain rate of 0.5 %/min. Figure 5 shows the cyclic behavior of the prestressed SMA wire which had a prestrain value of 6.4 %.

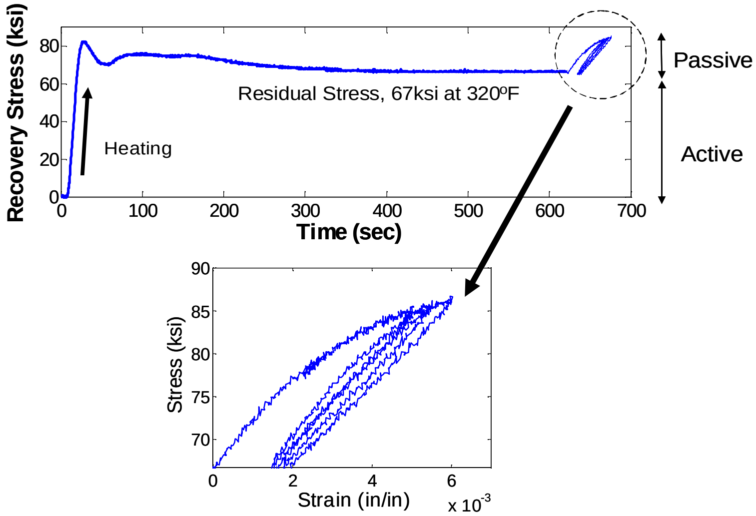

FIGURE 5 Cyclic behavior of prestressed SMA wire.

It might be important to note that prior to applying the cyclic load, the recovery stress developed in the wire will confine the concrete actively. However, when the concrete expands laterally under axial loading, additional passive confinement is provided by the SMA spiral as a result of the additional hoop stresses induced in the wires. Therefore, in real applications, the confining pressure provided by the SMA spiral is partially but dominantly active (prior to concrete loading) and partially passive (after concrete loading). The cyclic tests demonstrated that the confining stress induced in the SMA spiral is stable even when the concrete is subjected to cyclic loading such as in the case of seismic events.

3.2 CONCRETE CYLINDERS TESTS

Spirals made of NiTiNb SMA wires were utilized in this study to confine concrete cylinders. Due to shipping constraints, the SMA manufacturer was able to provide a maximum of 8-foot long segments of prestrained wires. Therefore, a splicing technique was established and tested to connect these segments in order to develop the full length of the spiral. Figure 6 shows a schematic of a typical SMA wrapped concrete cylinder that was used in the study. As illustrated in the figure, splicing connections were needed at the top and bottom loops of the spiral as well as at the location where two wire segments meet. In order to select a suitable connection for this application an experimental study was conducted.

To ensure that the selected connection will not fail prematurely during the testing of the cylinders, the used connection should be able to transfer force between the two connected wires greater than the recovery force and the force from passive effect from the wires (see. Figure.5). Figure 7 shows the three connection types that were considered in the study including: 1) Sleeve connection (Figure. 7a), 2) U-clamp connection (Figure. 7b), and 3) Welded connection, using metal inert gas (MIG) (Figure. 7c). The sleeve connection was tested with and without end stoppers. The first two types of connections were tested using different number of sleeves and U-clamps.

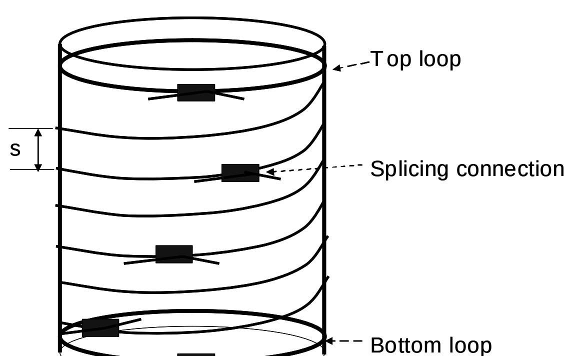

FIGURE 6 Concrete cylinder schematic showing the splicing connections used to develop the full length of the spiral.

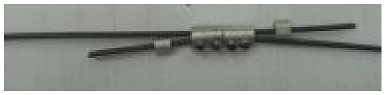

(a) Sleeve connection

(b) U-clamp connection

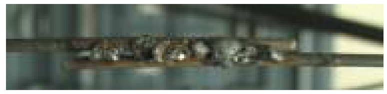

(c) Welded connection

FIGURE 7 Three types of splicing connections used in the study.

To examine the mechanical capacity of the connections, a tension test was conducted on the connections using the 20 kip MTS uniaxial servo-controlled hydraulic machine. The maximum stress that was developed in the wires prior to the failure of each connection was recorded. The connection which comprised four U-clamps was able to sustain a maximum force corresponding to a stress equal to 83.2 ksi, which was close enough to the ultimate stress (see Figure. 5). However, the maximum stresses developed in the wires in the cases of the sleeve and welded connections were 57.0 ksi and 11.2 ksi, respectively. Therefore, based on these results, the connection with the four U-clamps was deemed suitable for the proposed application and thus was used throughout the rest of the study.

The feasibility of the newly developed confinement concept using SMA spirals was first examined on the material level by conducting uniaxial compression tests on confined concrete cylinders. A number of 6 in. x 12 in. concrete cylinders were cast and cured in a moisture controlled room in preparation for testing. A 600 kip MTS uniaxial servo-controlled hydraulic machine was used to conduct the uniaxial compression tests with a loading rate of 0.04 in./min at room temperature. Averaging and circumferential extensometers were attached to the surface of the cylinders to measure the concrete axial and diametric strains, respectively. Three types of wraps were used in the study: (1) SMA spirals, representing the active confinement case. A spiral pitch spacing of 0.5 in. was used in this study, (2) SMA spirals plus Glass Fiber Reinforced Polymers (GFRP)/epoxy sheets (SMA-GFRP), representing a hybrid active/passive confinement case. Two pitch spacing values of 0.5 in. and 1 in. were used for the SMA spiral in conjunction with 2 and 4 sheets of GFRP, respectively, and (3) GFRP/epoxy sheets, representing the passive confinement case. The thickness of the GFRP sheets used in the study was 0.004 in. thickness. The hand lay-up method was utilized to apply the GFRP/epoxy sheets, which had a volumetric ratio in the range of 0.58 % to 2.86 %. The labels of the concrete specimens used in the study and their corresponding confinement methods are summarized in Table 1. In order to provide evenly distributed heating for the wrapped SMA spiral, an oven was utilized to heat the specimens gradually for 15 minutes until reaching a temperature of 320 ^{o}F. Tensile tests were also conducted on GFRP/epoxy coupons to determine their mechanical properties. The tests revealed an ultimate strain and Young's modulus of 0.018 in./in. and 2760 ksi, respectively.

TABLE 1 Specifications of the confinement techniques examined in the compression tests.

Specimen label	Confinement technique
Active-SMA	0.5 in.-pitch SMA spiral
Hybrid-1	1 in.-pitch SMA spiral + 2 layers of GFRP
Hybrid-2	0.5 in.-pitch SMA spiral + 4 layers of GFRP
Passive-1	2 layers of GFRP
Passive-2	4 layers of GFRP
Passive-3	8 layers of GFRP
Passive-4	10 layers of GFRP

In this stage, it was possible to heat the SMA spirals and to conduct the compression tests on the cylinders separately. Prior to conducting the compression tests, the prestrain losses that were experienced by the SMA spirals during heating were investigated. These losses could possibly take place as a result of geometric imperfection of the spiral that could cause the spiral to be slack and/or wire slippage that could occur at the splicing connections. The residual prestrain after all losses take place, will determine the effective amount of confining pressure applied on the specimens. Two extensometers were attached to the SMA spiral on opposite sides of the tested cylinders to monitor the

variation of the strain in the spiral. Table 2 presents a summary of the average values of prestrain losses for each of the tested specimens along with the corresponding maximum and residual recovery stress values. The average prestrain losses of Active-SMA, Hybrid-1, and Hybrid-2 specimens were 0.67 %, 0.33 % and 1.73 % respectively. The recovery stress values were obtained using the recovery stress versus prestrain relationships presented earlier in Figure 4.

TABLE 2 Prestrain losses (%) and recovery stress of concrete cylinders.

Specimen label	Avg. Prestrain losses (%)	Max. recovery stress (ksi)	Residual recovery stress (ksi)
Active-SMA	0.67	79.2	64.8
Hybrid-1	0.33	80.5	65.7
Hybrid-2	1.73	74.8	61.9

Figure 8 shows the Active-SMA specimen before, during and after testing. During testing, the concrete cylinder experienced significant cracking and crushing (see Figure 8b), however it remained intact because of the active pressure applied by the SMA spirals. After experiencing excessive deformations, the SMA spiral fractured suddenly and the cylinder failed diagonally as shown in Figure 8c. The stress-strain results obtained from the test is shown in Figure 9. The figure demonstrates that the performance of the concrete confined with the SMA spiral improved significantly in terms of strength and ultimate strain. Based on the recovery stress and prestrain loss values that were obtained earlier, the total confining pressure applied on the tested cylinder was approximately 206 psi. The peak strength of the confined concrete cylinder and the unconfined concrete cylinder were 6860 psi and 5686 psi, respectively, which indicates that the strength of the concrete confined with SMA spiral was approximately 21 % higher than that of the unconfined concrete. In addition, the ultimate strain of the SMA confined concrete was 24 times that of the unconfined concrete. The smooth and gradual softening of the stress-strain behavior during the post-peak phase of the Active-SMA specimen was due to the cracks which were slowly developing and progressing in the concrete. The active confining pressure applied by the SMA spiral was able to effectively control the opening and propagation of these cracks until the failure point (see Figure 8b). This is illustrated by the plateau which proceeded the softening branch. Even after the concrete had experienced severe damage, the SMA spiral was able to maintain about 55 % of the concrete's peak strength until failure occurred.

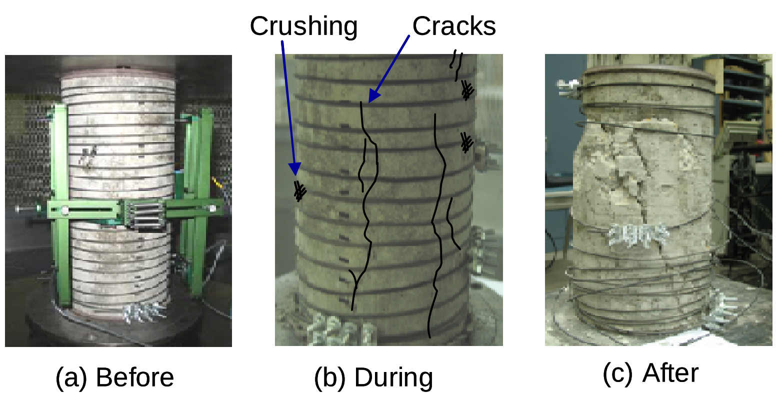

FIGURE 8 Active-SMA specimen before, during, and after compression test.

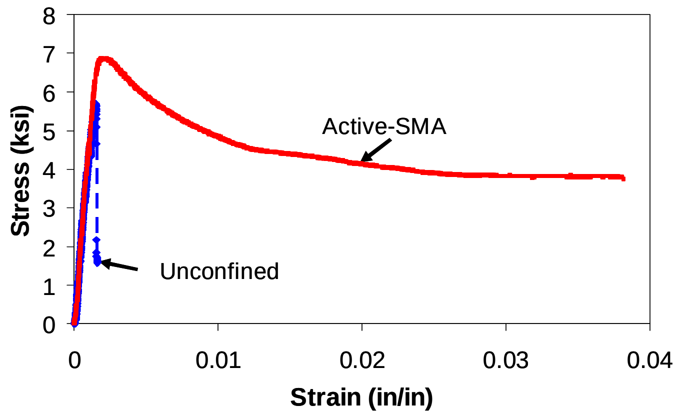

FIGURE 9 Compression stress-strain relationships of unconfined and Active-SMA specimens.

The effect of using a hybrid wrapping technique (SMA-GFRP) by combining passive and active confinement techniques was examined. The two specimens labeled Hybrid-1 and Hybrid-2 (see Table 2) were prepared using the hybrid wrapping technique and tested. Figure 10 shows the Hybrid-1 and -2 specimens before and after testing. Figure 11 shows the compression stress-strain behaviors of the concrete cylinders confined with the hybrid techniques. The peak strengths of the Hybrid-1 and Hybrid-2 specimens were 5961 psi and 6179 psi, respectively, which indicates an increase in the strength by 4.8 % and 8.7 %, respectively compared to that of the unconfined concrete cylinder. For both cases, Hybrid-1 and Hybrid-2, the hybrid technique improved the ultimate strain of the concrete cylinders dramatically by 30 and 25 times, respectively compared to that of the unconfined concrete. Observation of the specimens during testing revealed that the GFRP wraps started rupturing much earlier than the SMA spirals. The points of the rupture of GFRP in both cases are shown in Figure 11. After the GFRP wraps experienced severe damage, significant softening was observed followed by a slight strain hardening until failure. This strain hardening was a direct result of the contribution of the SMA spiral which solely dominated the behavior of the specimen after the GFRPs' rupture. Finally, the specimens reached their failure point when the SMA spirals fractured. It is clear from the behavior shown in the figure, that the SMA spiral played two important roles: 1) delay the rupture of the GFRP sheets, which was prestressed by the externally applied SMA spiral, and 2) act as a second line of defense which allowed the specimen to maintain an almost constant level of strength until failure.

(a) Hybrid-1 Before | (b) Hybrid-1 After | (c) Hybrid-2 Before | (d) Hybrid-2 After

FIGURE 10 Hybrid-1 and -2 specimens before and after compression test.

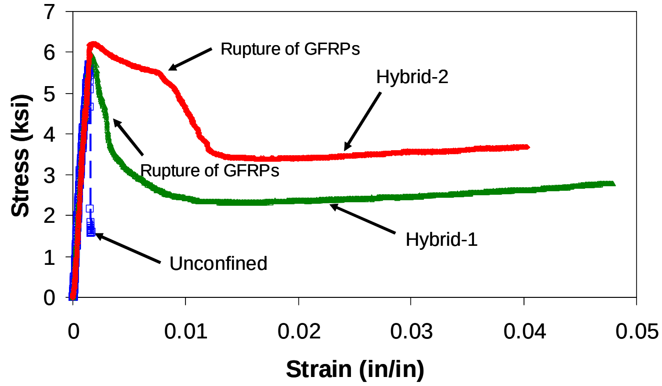

FIGURE 11 Compression stress-strain behaviors of unconfined and SMA-GFRP confined concrete cylinders.

For the purpose of comparison with the behavior of cylinders confined with SMA spirals, several concrete cylinders were tested in compression after being wrapped with GFRP/epoxy sheets. Using FRPs has been widely adopted in the field of retrofitting of RC structures as one of the superior passive confinement techniques, and also GFRP was especially selected in this study due to its relatively large ultimate strain. Table 3 presents the GFRP's volumetric ratio and the effective confining pressure corresponding to each of the tested specimens. The confining pressure was estimated at the onset of fracture of the wraps using the GFRP mechanical properties obtained from coupon tests after being reduced using an efficiency factor of 0.5. The efficiency factor value was based on previous studies*(3)* and is used to account for the imperfections in the GFRP wraps. The wrapped cylinders were tested using the same procedure that was previously described.

TABLE 3 Volumetric ratio and confining pressure of GFRP wrapped specimens.

Specimen label	r_{GFRP} (%)	Passive Confinement pressure (psi)
Passive-1	0.58	72.5
Passive-2	1.15	145
Passive-3	2.31	290
Passive-4	2.89	363

Figure 12 shows a comparison between the compression stress-strain behaviors of the concrete cylinders wrapped with different numbers of GFRP layers. As shown in the figure, the concrete strength and ultimate strain increased as the number of GFRP layers increased. However, the effect of confinement was more pronounced on the ultimate strain than on the strength. A minor change was observed in the strength in the case of the Passive-1 and Passive-2 cylinders, while in the case of Passive-3 and Passive-4, the concrete strength increased by 7 % and 18 %, respectively compared to that of the unconfined cylinder. The ultimate strain of the Passive-1, Passive-2, Passive-3 and Passive-4 specimens increased by 1.2, 2.1, 2.7 and 5.2 times, respectively compared to that of the unconfined concrete cylinder.

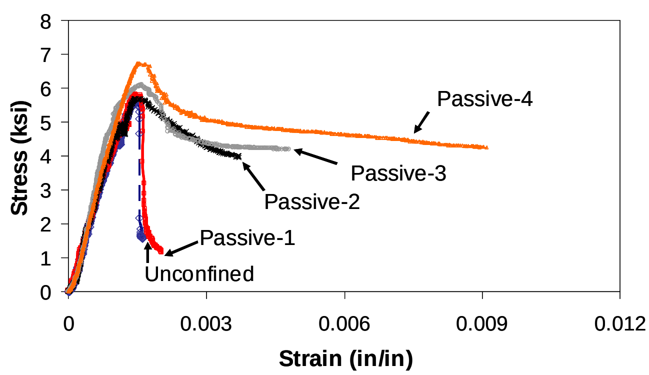

FIGURE 12 Comparison of the stress-strain behaviors of concrete cylinders confined with GFRP wraps.

As discussed earlier, the total confining pressure applied in the case of Active-SMA specimen was found to be 206 psi. This confining pressure falls between the 145 psi and 290 psi passive pressures applied in the cases of Passive-2 and Passive-3 specimens (see Table 3). Therefore, the stress-strain behaviors of the three specimens (i.e. Active-SMA, Passive-2 and Passive-3) were depicted on the same figure (see Figure 13) and compared. The figure shows that the active confining pressure improved the performance of concrete more dramatically compared to passive confinement. The strength of Active-SMA specimen increased by 21 % and 12 % compared to Passive-2 and Passive-3, respectively. In addition, the ultimate strain of Active-SMA specimen increased by 10 times and 8 times compared to that of Passive-2 and Passive-3, respectively.

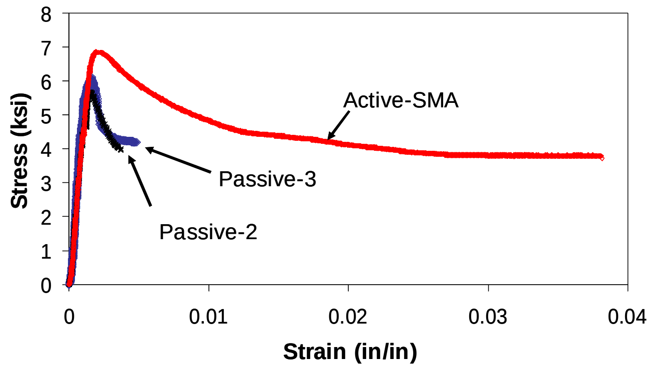

FIGURE 13 Comparison between the stress-strain behaviors of Active-SMA, Passive-2, and Passive-3 specimens.

For the cases of the Hybrid specimens, the total confining pressure was defined at the point where the GFRP starts rupture. Hence, at this point it is expected that the passive pressure applied from the SMA spiral is minimal, and thus the total confining pressure was determined as the summation of the active pressure from SMA spirals, and the passive pressure from GFRPs wraps. For the Hybrid-1 specimen, the total confining pressure was found to be 145 psi, which consisted of 72.5 psi applied as active pressure from the SMA spiral and 72.5 psi applied as passive pressure from the GFRP wraps at the onset of their rupture. The total pressure was equivalent to the passive pressure when using two layers of GFRPs, which was estimated as 145 psi (see Table 3). Therefore, the behaviors of the two specimens Hybrid-1, and Passive-2 are presented and compared in Figure 14. The behaviors were almost identical until the concrete cylinder confined with four layers of GFRP sheets failed, after which the behaviors were significantly distinguishable. The hybrid wrapping technique improved dramatically the concrete ultimate strain by approximately 13 times compared to the passively confined specimen. Although the Hybrid-1 specimen comprised half of the GFRP wraps used in the Passive-2 specimen, the GFRP rupture point for both specimens were almost identical. This demonstrates the effectiveness of the SMA spiral in delaying the rupture of the GFRP wraps used in the hybrid specimen. The brittle behavior of the GFRP wraps limited the ability of the Passive-2 specimen to maintain any residual strength. However, the active confining pressure provided by the SMA spiral exhibited an effective role in controlling the residual strength which was almost maintained at a level of 46 % of the peak strength.

On the other hand, in the case of the Hybrid-2 specimen, the total confining pressure was found to be 305 psi, which comprised 160 psi active pressure and 145 psi passive pressure. This total confining pressure was comparable to the passive pressure of 290 psi, which was obtained from using eight layers of GFRPs (see Table 3). Therefore, the behaviors of the Hybrid-2 and Passive-3 specimens are presented and compared in Figure 14 as well. In terms of the peak strength, the two specimens were almost identical, however, in terms of the ultimate strain, the hybrid technique showed a superior performance to the traditional passive confinement technique. The ultimate strain of the Hybrid-2 specimen was 9 times that of the Passive-3 specimen. One noticeable observation was that eight layers of GFRP (represented by Passive-3) reached their rupture strain much earlier than the four layers of GFRP used in the Hybrid-2 specimen due to the prestressing effect of the SMA spirals. Furthermore, the SMA spiral was successful in maintaining about 60 % of the concrete peak strength until failure.

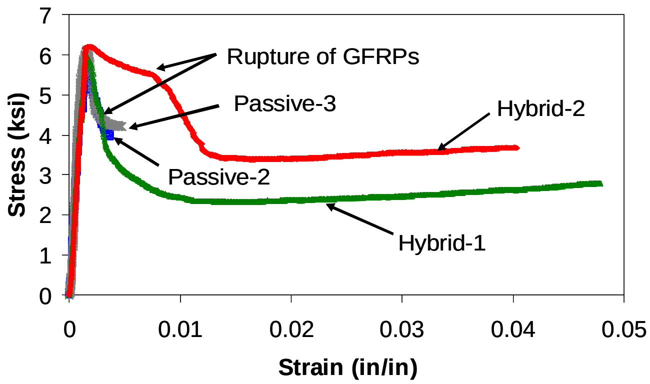

FIGURE 14 Comparison between the stress-strain behaviors of cylinders confined using hybrid and passive confinement methods.

3.3 REINFORCED CONCRETE COLUMNS TESTING

3.3.1 Specimen Description

To study the new retrofitting concept on the structural component level, four reduced-scale RC single cantilever columns were built and tested under quasi-static lateral cyclic loading. Figure 15 shows pictures of the column reinforcement, casting, and finished column specimen. And Figure 16 shows an isometric view and a schematic elevation of the column. The effective height of the column was 55 in., and its diameter was 10 in. with 1 in. concrete cover. The column was supported by 46 in. x 46 in. x 16 in. footing. To mimic the effect of static gravity loads, the axial force in the column was maintained at a value of 25.3 kips during testing, which represents 5 % of the column's compressive strength. The axial force was applied using a 100 kip hydraulic actuator mounted on the top of the column and anchored to a 0.6 in. seven wire steel strand. The column was reinforced by 8#4 bars in the longitudinal direction and #2@4 in. hoops placed in the transverse direction. The longitudinal reinforcements were designed to represent 2 % of the volumetric ratio, and the transverse reinforcements were chosen to represent a poor condition of transverse reinforcements used in the RC columns built according to old seismic design provisions. Four Linear Variable Differential Transformers (LVDTs) were installed to measure the net displacements of the column. The lateral force was applied using a 100 kip servo-controlled hydraulic actuator with a stroke of ± 10 in. The actuator was anchored to the reaction wall using a steel block and a concrete block as shown in Figure 16. At the time of testing, the average compressive strength of the concrete was found to be 6500 psi.

(a) Details of reinforcements

(b) Pouring the concrete

(c) As-built Column

FIGURE 15 RC column specimen.

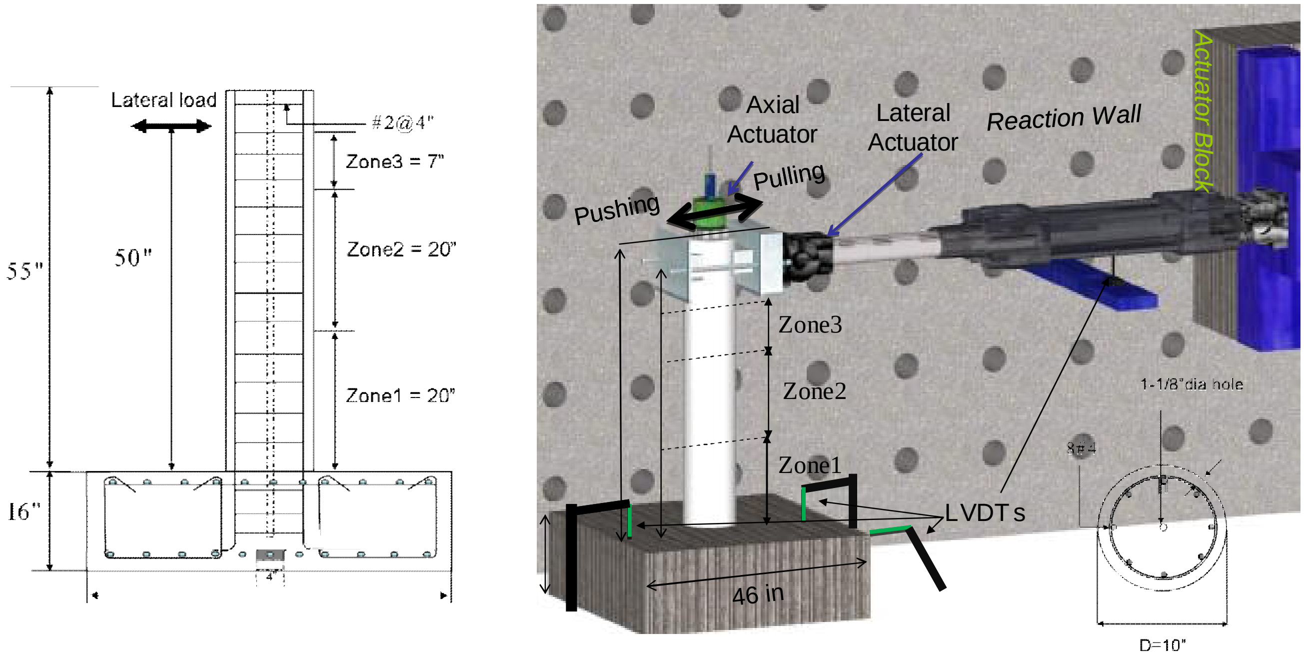

FIGURE 16 Schematic of the RC columns used in the tests.

Three of the columns were retrofitted using a different confining technique while the fourth column was tested in its as-built condition and used as a basis for the comparison. Figure 17 shows the four columns before testing. The retrofitted columns were divided into three regions as shown in Figure 16. One column was retrofitted entirely with GFRPs, while two columns were retrofitted with NiTiNb SMA spirals at the plastic hinge zone. One of these two columns was wrapped with GFRP sheets in addition to SMA spirals. The SMA spirals were heated by passing an electrical current and then using a fire torch. Based on the material tests presented earlier, the hybrid confinement technique showed very promising results. Therefore, it was decided to continue investigating it on the structural component level.

Table 4 shows a summary of the confinement techniques used for each column at Zone 1, 2, and 3. For consistency, all three retrofitted columns were wrapped with the same number of GFRP sheets (0.004 in.-thick) at Zone 2 and 3; five sheets at Zone 2 and two sheets at Zone 3. However, Zone 1 (plastic hinge zone) was retrofitted differently in the three columns. For the GFRP retrofitted column, Zone 1 was wrapped with 10 layers of GFRP; while for the SMA column, 0.08 in. NiTiNb SMA wire was used as a spiral with 0.4 in. pitch. Based on the previously discussed mechanical properties of the GFRP and using a jacket efficiency factor of 0.5 *(3)*, the predicted confinement pressure corresponding to 10 layers of GFRP was 218 psi. Using the SMA recovery stress results (see Figure 3 and 4), the pitch of the SMA spirals was determined so that the spiral would exert the same confinement pressure at Zone 1 as that of the 10-layer GFRP jacket. The amount of SMA and GFRP was cut into half for the hybrid column (i.e. 5-layer GFRP jacket + SMA spiral w/0.8 in. pitch), which resulted in half of the confinement pressure being applied actively, while the other half applied passively.

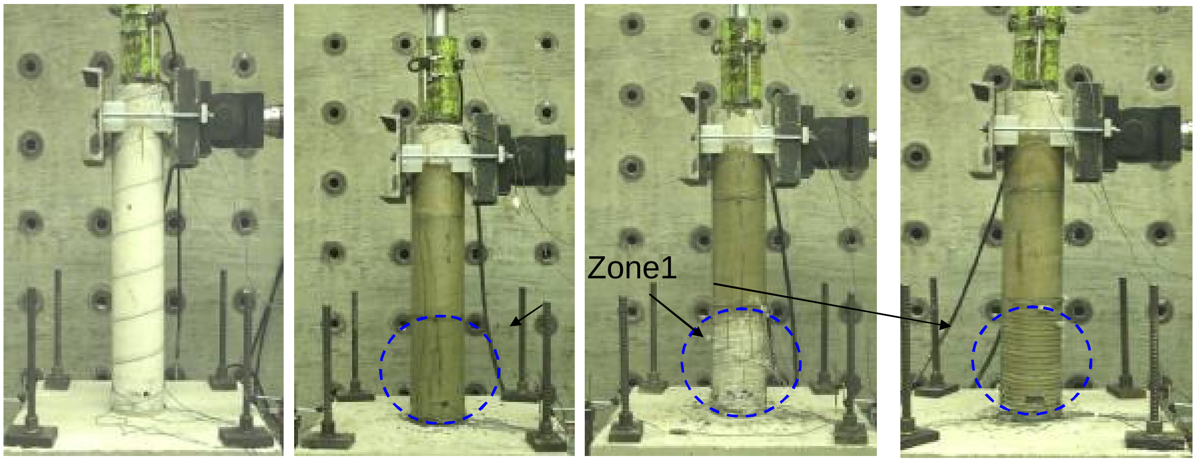

FIGURE 17 Four column specimens before testing.

TABLE 4 Confining techniques at each column

Specimen	Zone 1	Zone 2	Zone 3
GFRP Column	10-layer GFRP jacket	5-layer GFRP jacket	2-layer GFRP jacket
SMA Column	SMA spiral w/0.4 in. pitch	5-layer GFRP jacket	2-layer GFRP jacket
Hybrid Column	SMA spiral w/0.8 in. pitch + 5-layer GFRP jacket	5-layer GFRP jacket	2-layer GFRP jacket

3.3.2 Loading Protocol

Figure 18 shows the load protocol that was used in the tests. The columns were loaded cyclically with a rate of 0.2 in./min up to 1.5 % drift and 0.6 in./min thereafter. Initially a load increment of 0.5 % drift was adopted until a drift of 6 % was reached, after which an increment of 1 % was used until 12 % drift, followed by an increment of 2 % until the end of the test.

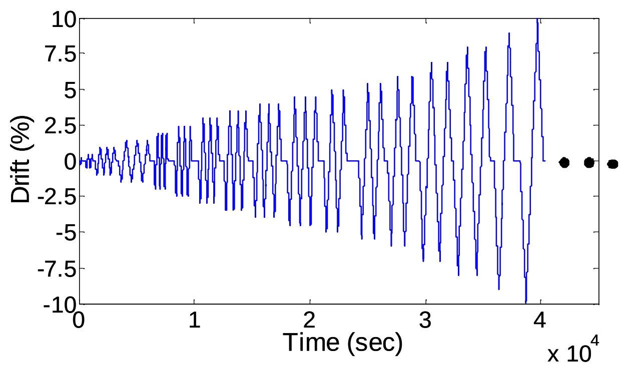

FIGURE 18 Loading protocol used in the study.

3.3.3 Test Results

Figure 19 shows the lateral force versus lateral drift of the four tested columns. The columns retrofitted with SMA spirals were able to sustain larger force and drift and dissipate significantly more hysteretic energy compared to that of the as-built and GFRP column. The yielding of the longitudinal steel in the as-built column was first observed at 1.5 % drift ratio and the column reached a maximum strength of 7.76 kips at 2.8 % drift ratio. For the GFRP retrofitted column, the

maximum strength recorded was 7.89 kips at a drift ratio of 3.5 %. After which the column started showing signs of gradual strength degradation. At 8% drift, the strength was reduced to 34.6 % of the maximum strength. The maximum strength of the SMA column was found to be 8.27 kips at 12 % drift ratio. After steel yielding, hardening behavior was observed. The Hybrid column had the maximum strength of 8.00 kips at the 10 % drift ratio. For the SMA and hybrid columns, hardening behavior was observed after steel yielding. This could be attributed to the elastic behavior of the SMA spirals. The test of the SMA retrofitted columns was stopped when the load-carrying capacity degraded by approximately 20 % of the maximum strength. The strength degradation was due to the rupture of one of the longitudinal reinforcement bars. The longitudinal reinforcement bars of the SMA and Hybrid columns ruptured at 12 % drift and 10 % drift, respectively.

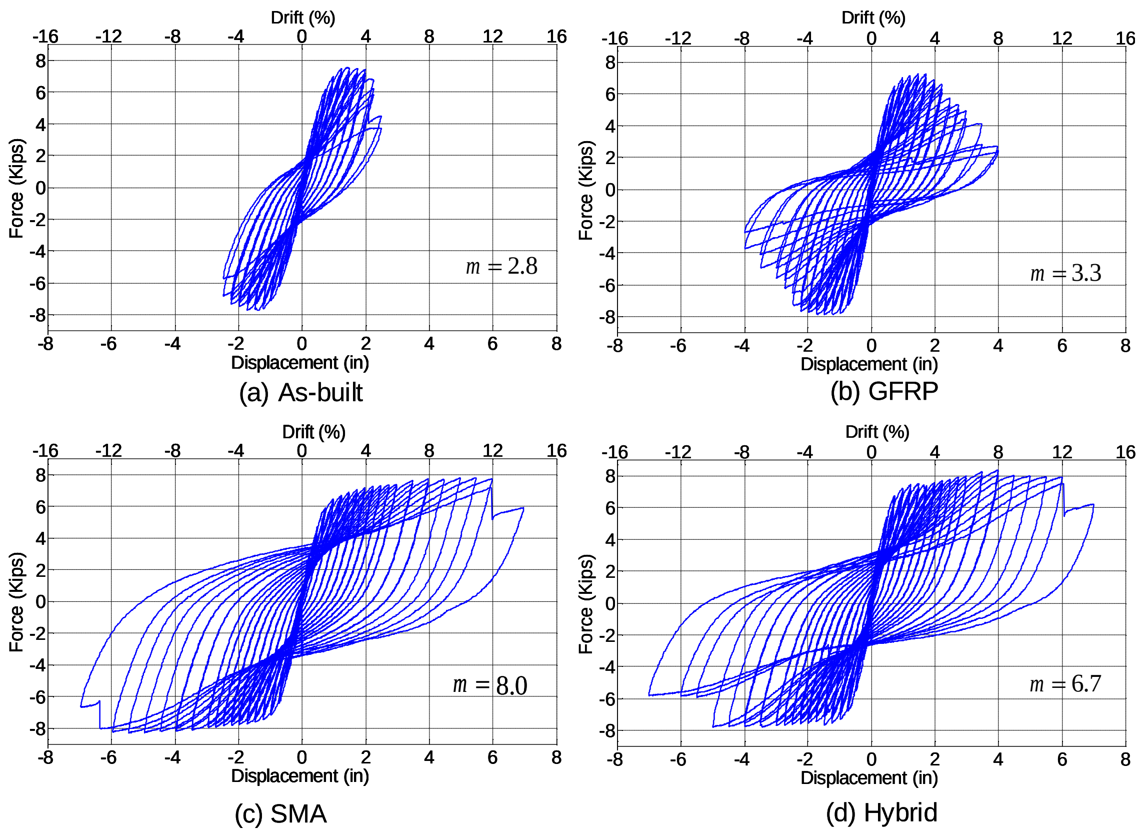

FIGURE 19 Lateral force vs. lateral drift of the four tested columns.

The displacement ductility ratios (μ) of the four columns were computed to evaluate and compare their flexural ductility capacity. The ductility ratio is defined as the ratio between the drifts at the ultimate point (measured at 80 % of the ultimate strength) and the yielding point. Based on this definition, the ductility ratios of the As-built, GFRP, SMA, and hybrid columns were 2.8, 3.3, 8.0, and 6.7, respectively. A summary of the strength and ductility ratio results is presented in Table 5 showing the strength and ductility ratio normalized values based on the as-built column results. The conventional passive confinement technique using GFRP wraps increased the strength and the ductility by 2 % and 18 %, respectively. However, the columns retrofitted with SMA spirals showed 3~7 % increased strength, and 139 %~185 % increased ductility compared to the as-built column. Furthermore, the GFRP retrofitted column started showing significant signs of stiffness degradation and strength deterioration at a drift ratio of 5 %, while in the case of the SMA retrofitted columns, no signs of degradation were observed until the column reached a drift ratio of 12 % (SMA column) and 10 % (Hybrid column).

TABLE 5 Maximum and normalized strength and ductility of the four columns

	As-built	**GFRP**	**SMA**	**Hybrid**
Max. Strength (kips)	7.76	7.84	8.27	8.00
Normalized Strength	1	1.01	1.07	1.03
Ductility Ratio	2.8	3.3	8.0	6.7
Normalized Ductility Ratio	1	1.18	2.85	2.39

3.3.4 Evaluation of Damage

In addition to improving the column ductility, it is important for the retrofitting method to limit the damage sustained by bridge column during major seismic events. This will ensure that the functionality of the transportation network will not be disrupted after an earthquake. The effectiveness of the new retrofitting technique using SMA spirals was evaluated after the columns were tested. Figure 20 shows the damage sustained by the four columns at a drift ratio of 8 % except the as-built column, which was tested until 5 % drift. For the as-built column, the column was severely damaged, having completely spalled cover concrete, heavily crushed core concrete, and ruptured and buckled reinforcement bars at the 5 % drift ratio (see Figure 20.a.). Also it could be seen from the figure (see Figure 20.b) that at 8 % drift, the GFRP retrofitted column sustained significant damage in the form of rupture of GFRP sheets, complete spalling of the concrete cover, and significant crushing of the concrete core. However, for the case of the SMA and the hybrid columns, only minor damage in the form of horizontal cracks in the concrete cover or GFRP jacket was observed (see Figure 20.c and d). This limited damage could be attributed to the large active confining pressure applied by the SMA spirals, which helped in delaying the crushing of the concrete underneath.

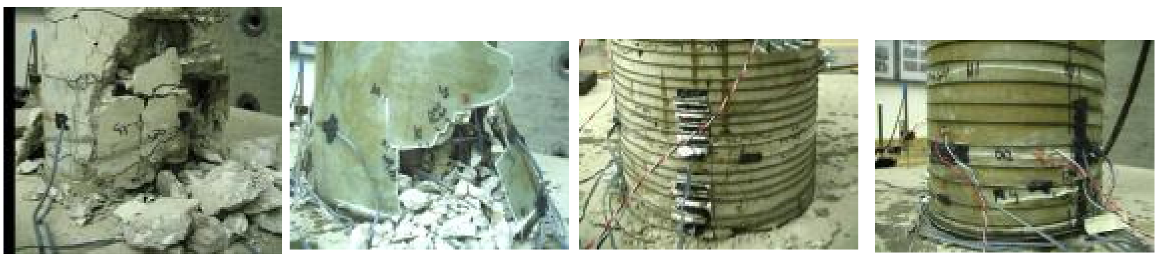

a) As-built b) GFRP c) SMA d) Hybrid

FIGURE 20 Damage sustained by the as-built column at 5 % drift (a) and retrofitted columns (b), (c), and (d) at 8 % drift

Figure 21 shows the four columns after removing the wrappings and cleaning up the crushed concrete. As indicated earlier, the final drift ratios sustained by the columns were 5 %, 8 %, 14 % and 14 % for the as-built, GFRP, SMA and hybrid columns, respectively. As shown in the figures, the as-built and GFRP columns sustained severe and irreparable damages. Even though during testing the SMA and hybrid columns reached 75 % more drift than the GFRP column, their level of damage was extremely less than that of the GFRP column. This clearly demonstrated that using SMA spirals is not only effective in improving the flexural ductility of the columns, but also in limiting their damage during earthquakes, which will have a significant impact on maintaining the post-earthquake bridge functionality.

a) As-built b) GFRP c) SMA d) Hybrid

FIGURE 21 Damage sustained by the four columns after the GFRP sheets and SMA spirals are removed.

4. PLANS FOR IMPLEMENTATION

This project helped in proving the concept of using thermally prestressed SMA spirals for retrofitting vulnerable RC bridge columns. The product (i.e. SMA spiral) is ready for immediate use in retrofit and emergency repair projects. Although the project has ended, work is still underway to provide the bridge engineering community with more data and information on the behavior and longevity of these spirals when used in real bridges. Among the issues which are currently being investigated is:

- Understanding the behavior of the spirals and the actively confined concrete under real seismic loading (i.e. strain rate effects).
- Studying the durability of the spiral under harsh environmental conditions.
- Searching for other cost-effective SMAs with thermomechanical characteristics suitable for the application of interest.
- Modeling the behavior of the actively confined concrete using SMA spirals. This will help in studying the impact which this new retrofitting/repair technique has on the entire bridge system.
- Studying the feasibility of using the same concept studied in this project in retrofitting/repairing non-circular columns.

5. CONCLUSIONS

This project explored a new application of SMAs that could potentially transform how RC bridges are retrofitted and/or repaired. The results of the project clearly proved the superiority of the proposed SMAs spirals compared to the currently used FRP jackets in terms of: (1) Increasing the flexural ductility of the columns (more than 2.4 times the ductility obtained from using GFRP jacket). (2) Limiting the damage sustained by the columns even under excessive lateral drifts (14 %-drift). Furthermore, the amount of SMA used to reach such superior behavior was relatively small and the amount of time and labor required for installing the SMA spirals were minimal. Unlike using prestressed strands or FRP jackets, installing the thermally prestressed SMAs will require minimal labor and hardware. Further, in contrary with FRP jackets, the proposed SMA spirals do not require any curing time, which makes the spirals very suitable for emergency repairs following a major earthquake or a collision accident. This project has provided bridge engineers with an effective and easy tool for applying the concept of active confinement on-site. This very concept can be used to mitigate the effects of various man-made and natural hazards (e.g. earthquakes, impacts, blasts, etc.) on bridges.

6. REFERENCES

1. Richart, F.A., Brandtzaeg, A. and Brow, R. L. A study of the failure of concrete under combined compressive stress. Bulletin 185, University of Illinois Engineering Experiment Station, Urbana IL, 1928.

2. Otsuak, K., and Wayman, C.M. Shape memory material. *Cambridge University Press*, New edition, 2002.

3. L.D. Lorenzis and R. Tepfers. Comparative Study of Models on Confinement of Concrete Cylinders with Fiber-Reinforced Polymer Composites. J.Composite for Construction. ASCE, Vol. 7, No. 3, 2003, pp. 219-237.